



UNIVERSITI  
TEKNOLOGI  
PETRONAS

Mechanical Design and Dynamic Analysis of Pipe Crawling Robot for  
Internal Gas Pipeline Inspection

Muhammad Nor Hakim bin Mohd Arif

Mechanical Engineering

Universiti Teknologi PETRONAS

MAY 2013

**Mechanical Design and Dynamic Analysis of Pipe Crawling Robot for Internal Gas Pipeline Inspection**

by

Muhammad Nor Hakim bin Mohd Arif

Dissertation submitted in partial fulfilment of  
the requirements for the  
Bachelor of Engineering (Hons)  
(Mechanical Engineering)

MAY 2013

Universiti Teknologi PETRONAS  
Bandar Seri Iskandar  
31750 Tronoh  
Perak Darul Ridzuan

CERTIFICATION OF APPROVAL

**Mechanical Design and Dynamic Analysis of Pipe Crawling Robot for Internal  
Gas Pipeline Inspection**

by

Muhammad Nor Hakim bin Mohd Arif

A project dissertation submitted to the  
Mechanical Engineering Programme  
Universiti Teknologi PETRONAS  
in partial fulfilment of the requirement for the  
BACHELOR OF ENGINEERING (Hons)  
(MECHANICAL ENGINEERING)

Approved by,

---

(Dr Mark Ovinis)

UNIVERSITI TEKNOLOGI PETRONAS  
TRONOH, PERAK  
MAY 2013

## CERTIFICATION OF ORIGINALITY

This is to certify that I am responsible for the work submitted in this project, that the original work is my own except as specified in the references and acknowledgements, and that the original work contained herein have not been undertaken or done by unspecified sources or persons.

---

(MUHAMMAD NOR HAKIM BIN MOHD ARIF)

## **Abstract**

Pipelines play an important role in terms of transporting various types of fluid like liquid and gas. They are mainly used not only in small applications like housing area, but also in large industrial field like in an oil and gas field. Maintenance of these pipelines is crucial and the cost of doing it continues to increase from time to time and thus a new approach is needed in order to tackle these problems. This project report presents the design and development of crawling robots for internal pipe inspection. There are four designs being considered but this paper will present the simplest of the design which is the wheeled type design that with a pantograph mechanism with a sliding base that allows folding and unfolding of the robot's legs. The mechanism of this robot is based on the design of MRINSPECT III and the driving mechanism of MRINSPECT IV. The robot is designed accordingly so that it can function through a pipeline ranging from 6 inches diameter to 10 inches diameter. The design is then modeled and simulated using AutoCAD and ADAMS respectively.

## **Acknowledgement**

First and foremost I would like to express my deepest gratitude to my supervisor, Dr. Mark Ovinis who has guided, supported and encouraged me to successfully complete this project. He has always given me great advices and suggestions and he also expects something great from this project. He has also given motivations and directions whenever I was lost upon completing this project.

Not to forget to Mr. Muhaimin who has taught me on doing the ADAMS View Software. He has helped me throughout the simulation process of the project. Last but not least, special thanks to family, friends and others who had directly or indirectly involved in helping me to complete this project.

## Table of Contents

<b>Certification of Approval</b> .....	ii
<b>Certification of Originality</b> .....	iii
<b>Abstract</b> .....	iv
<b>Acknowledgement</b> .....	v
<b>Chapter 1: Introduction</b> .....	1
1.1 Background Study.....	1
1.1.1 Gas Pipeline.....	3
1.1.2 Pipe Crawling Robot.....	2
1.2 Problem Statement.....	3
1.3 Objectives.....	3
1.4 Scope of Study.....	3
<b>Chapter 2: Literature Review</b> .....	4
2.1 Driving Mechanism.....	4
2.1.1 General configuration of In-pipe Robot.....	5
2.1.2 Design of In-pipe Robot According to Fittings.....	5
2.1.3 Wheeled Type Design.....	5
2.1.4 Wheeled Type Design with Tilted Wheels.....	10
2.1.5 Inchworm Type Design.....	12
2.1.6 Snake and Legged Robot.....	14
2.1.7 Size of the Robot.....	15
2.2 Summary.....	16
<b>Chapter 3: Methodology</b> .....	17
3.1 Project Activity.....	17
3.1.1 Literature Review.....	17
3.1.2 Design and Modeling.....	17
3.1.3 Simulation.....	18
3.2 Gantt Chart.....	21
<b>Chapter 4: Results and Discussion</b> .....	25
4.1 Robot's Design and Development.....	25
4.1.1 Robot's Mechanism.....	25
4.1.2 General Dimension of the Robot.....	27
4.1.3 Spring Design.....	30
4.1.4 Driving Mechanism.....	33
4.2 Design Models.....	34
4.3 Simulation.....	35
4.3.1 Spring Deformation and Forces.....	35
4.3.2 Forces Acting on Each Joint.....	37
4.3.3 Velocity.....	44
<b>Chapter 5: Conclusion and Recommendations</b> .....	45
<b>References</b> .....	46
<b>Appendices</b> .....	49

## List of Figures

Figure 1 Classification of In Pipe Robots. (a) Pig type. (b) Wheel type. (c) Inchworm type. (d) Caterpillar type. (e) Screw type. (f) Walking type. (g) Wall press.....	4
Figure 2 MRINSPECT in pipe robot (a) and its basic mechanism (b).....	7
Figure 3 MRINSPECT II (a) and its corresponding mechanism (b).....	7
Figure 4 MRINSPECT IV (a) and its corresponding mechanism (b).....	8
Figure 5 The 3D model of components of minirobot .....	8
Figure 6 Elementary mechanism (a) and the structural scheme of the minirobot (b).....	9
Figure 7 Transmission with gears in the structure of the minirobot .....	9
Figure 8 Robot architecture. Two body architecture .....	10
Figure 9 Three body architecture for smaller diameter.....	11
Figure 10 Extensor module (a) main components. (b) Power transmission (c) Continuum links and its linear motion.....	13
Figure 11 Upper clamper module. (a) Main components of clamper module. (b) Crank-slider mechanism .....	14
Figure 12 Size of the robot (a) Negotiating with the elbow (b) Negotiating with the branch	15
Figure 13 Process flow of the project .....	20
Figure 14 Kinematic Diagram of MRINSPECT III.....	26
Figure 15 Side View of One of the Legs .....	29
Figure 16 CAD model of the main body frame .....	29
Figure 17 Spring Design .....	32
Figure 18 Spring attachment to the main body frame.....	32
Figure 19 Driving Modules with sets of gears .....	33
Figure 20 Robot's model in 10 inches diameter.....	34
Figure 21 Robot's model in 6 inches diameter.....	34
Figure 22 Spring deformation VS Time .....	35
Figure 23 Forces against Pipe Radius .....	36
Figure 24 Kinematic Diagram with Joints .....	38
Figure 25 Velocity against Time.....	44

## **Chapter 1: Introduction**

### **1.1 Background Study**

#### **1.1.1 Gas Pipelines**

In this modern world, pipeline is widely used with numbers of function like transporting and conveying water, gas and other fluid. The applications of these pipelines can be seen anywhere from home use to industrial use like in the oil and gas field. Like any other structure available today, these structures are vulnerable to damage and it comes from many factors like chemical factors such as corrosion and physical impact (W. Jeon, J. Park, I. Kim, Y.K. Kang, and H. Yang, 2011). These damages are harmful as it can threaten the safety of humans in industrial fields. Smaller fluid systems such as those serving in housing areas may be repaired with minimal costs and even in some cases the best way is to replace the whole piping systems. But in bigger industrial fields like oil and gas field which has complex pipelines system, a better way of dealing with these problems has to be performed. This is because in general, gas pipelines are installed where normal human beings can hardly get access to, such as underground. Even though the underground pipes can be inspected, it is not as efficient as inspecting them above-ground. This is because of the excavation and backfilling work involved <sup>[8]</sup>.

Numbers of methods and solutions are done to inspect pipelines that are hard to reach by humans. One of the methods is called by using a passive device called Pipe Inspection Gauges (PIG). The PIG which is sent through the buried pipe for inspection and cleaning purposes are designed a positive obstruction can be provided within the interior surface of the pipe. The PIG is driven by giving pressure in the direction of the desired direction <sup>[12]</sup>.

Another method that is used to perform interior pipe inspection is ultrasonic sensors to detect cracks or corrosion thinning in pipes. Though this method is proved to be efficient, it requires access to the external surface of the pipes and this is difficult considering the duration and most importantly, cost. So in this case, an internal pipeline inspection may be the best ways to prevent the problems

### **1.1.2 Pipe Crawling Robots**

Robotics is one of the fastest growing engineering fields today (O. Tatar, D. Mandru, I. Ardelean, 2007). They are designed to ease humans from performing dangerous tasks and works and also to act in an unreachable environment. Nowadays the use of the robots are much more common than ever as the technology is growing and thus heavy production industries are growing. It is also one of the most attractive solutions available because the usage of a robot is less costly and can be handled easily.

There are numbers of researches have been done on in-pipe inspection robots (W. Jeon, J. Park, I. Kim, Y.K. Kang, and H. Yang, 2011). It was found that there are several types of mechanisms that have been developed on pipe inspection robots. These designs can be distinct from each other in term of moving mechanisms, for example there are some using wheel types, crawler type and inchworm type. Some of these robots have also been used in actual application. These robots must be able to do inspection in many types of pipes as they are not necessarily installed horizontally. Some pipes are installed vertically with branches, junctions and curves.

Among the designs of the in-pipe inspection robots, the wheeled type robot is the simplest one. These types of robots have the advantage of easier miniaturization<sup>[1]</sup>. These types of robots also have more or less complicated kinematical structures, depending on the diameter adaptability and turning capability<sup>[2]</sup>.

## **1.2 Problem Statement**

Gas pipelines networks, like any other structure, are vulnerable to damage from various sources: aging, corrosion, cracks, mechanical damages. It is possible to detect cracks or corrosion thinning in plumbing with various methods of non-destructive testing such as eddy-current or ultrasonic sensors. However these require access to the outside of the pipes which is difficult and costly in many situations due to long and buried lengths. Furthermore, this does not address the problem of clogging or fouling. In many such applications, an internal inspection solution may be preferable. Numerous pipe-inspection robots have been constructed and have shown promise but remain experimental.

## **1.3 Objectives**

The main objectives of this project are to design, develop, simulate and analyse a pipe crawling robot for internal pipeline inspection with inside diameters ranging from 6 to 10 inches.

## **1.4 Scope of Study**

- The scope of the project is only focused on mechanical and structural design including the driving mechanism of the pipe crawling robot. The robot must have the following features:
  - It has a very simple structure (i.e., the minimum number of moving parts/actuators).
  - It is stable enough, throughout its motion, to maximize the performance of the inspection sensors.
  - It can suit pipes with inside diameters ranging from 6 to 10 inches.
- The project is targeted to build and design a functional robot where the application can be tailored to internal pipelines inspection and maintenance.

## Chapter 2: Literature Review

### 2.1 Driving Mechanism

In this modern day, the applications of robots for the maintenance of the pipeline utilities are considered as one of the most attractive solutions available in inspecting pipelines conditions <sup>[7]</sup>. The design of the in-pipe inspecting robot have long been studied and produced and they are classified into several elementary forms according to the patterns of movements of the robot as shown in the Figure even though they are designed depending upon specific applications.

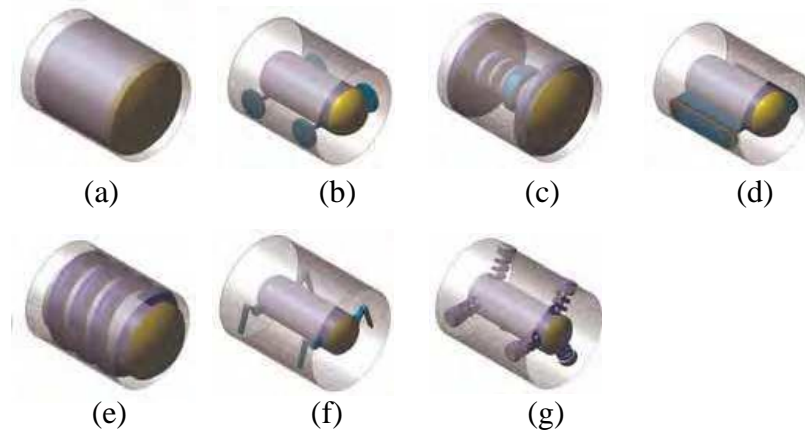


Figure 1 Classification of In Pipe Robots. (a) Pig type. (b) Wheel type. (c) Inchworm type. (d) Caterpillar type. (e) Screw type. (f) Walking type. (g) Wall press

#### 2.1.1 General Configuration of In-Pipe Robot

Generally, in-pipe robot consists of articulated bodies including driving vehicles, control module, tether cable and ground station <sup>[7]</sup>. Depending on the designer, Non Destructive Testing (NDT) can be attached to the body of the robot. Figure shows the possible configuration of the robot comprising of functionally partitioned modules such as driving modules, control modules and NDT modules.

Principally, the robot is designed to have sufficient traction forces to climb he vertical pipelines or pull the tether cables, which are provided by two driving vehicles in front and rear of the robot <sup>[7]</sup>. In every vehicle of the robot there will be flexible wheeled leg mechanisms pressing the wall. This results in the the generation

of the forces due to the friction between the wheels and the inside wall of the pipelines. The driving vehicle located in front of the robot generates traction forces and pushing forces are generated by the vehicle in the rear sides. The in-pipe robot communicates with the ground station by specially designed tether cable <sup>[7]</sup>.

### **2.1.2 Design of In-Pipe Robot According to Fittings**

The shape and the size of the robot are one of the most important aspects that have to be considered in defining the maneuverability of a robot as it depends on the pipeline configuration. Pipelines are basically installed in a horizontal and vertical position. They also have branches, junctions and elbows and some other unexpected mechanical damages such as dents, gouges, and the removed metals caused by third parties <sup>[7]</sup>. In a nutshell, to design a robot, these considerations and requirements can be derived as follows;

- Active steering capability in branches <sup>[7]</sup>
- Surmounting right angle elbow <sup>[7]</sup>
- Driving through pipelines with a various diameter ( $\pm 20\%$ ) <sup>[7]</sup>
- Sufficient traction forces (vertical load excluding self-weight) <sup>[7]</sup>

Like mentioned before, numbers of designs have been developed based on the requirements stated above and they have different mechanisms and structures. The next part of this report will discuss on the different designs developed by some engineers all over the world.

### **2.1.3 Wheeled-type Design**

For in-pipe inspection robots, there are numbers of design and mechanisms available, from wheel type mechanisms to inchworm type mechanisms. These designs have their own advantages and disadvantages as they are restricted and the designs of the robots must be able to navigate and carry on the tasks of inspecting in cylindrical space. Furthermore, the pipes are not necessarily straight. There are various types of pipes such as curved and branch pipes and these are installed wither

vertically or horizontally. Also, the robots must be able to overcome numbers of technical difficulties associated with the change in diameters of the pipes, curves and energy supply.

One of the simplest designs for in-pipe inspection robot is the wheeled type robots <sup>[1]</sup>. The wheeled type robots have the best potential for long range pipe, as well as the most energy efficient. In addition, the benefit of having a wheeled type inspection robot is that the design has the advantages in maneuverability as it has the ability to adapt to uneven surfaces, move vertically in pipes and stay stable without slipping in pipes. Due to their simple design, the control procedures, good energy efficiency and miniaturization potential, the wheeled type robot are commonly used in the field of pipe inspection robot <sup>[1][1]</sup>.

The wheeled type robots have similar behavior of any wheeled type vehicles in which they depend on their own weight to provide continuous contact between the wheels and the surface of the pipe <sup>[11]</sup>. Some of the robots that apply the pressing of wheels to the surface of the internal pipes are the robots seen in (Kawaguchi et al. 1995; Tache et al. 2007) <sup>[11]</sup>. These robots completely depend on magnetism, which is used to attract the wheels to the surface of the pipe wall so that the robots would not be swept away in case of high rates fluid flow. Even though this design does not have any restriction in terms of pipe diameters, the use of the magnets will only limit them to the pipe that is of ferrous materials.

Numbers of wheeled type in-pipe inspection robot have been developed and they have different means of operation like passive means (e.g. spring), or active means (e.g. linear actuators), or a combination of both <sup>[11]</sup>. Examples of such robots that possess such designs and mechanisms are the MOGRER by Fujiwara, the screw-drive robot presented in Peng Li's paper and the MRINSPECT series of robots. Even though these robots have different designs they use a common principle of pushing the wheels against the inner surface of the pipe <sup>[11]</sup>.

Figure 1 shows the designs of wheeled type in-pipe inspection robots by O. Tatar, D. Mandru and I. Ardelean. The robots are called MRINSPECT (*Multifunctional Robotic crawler for INpipe inspection*) <sup>[6]</sup>. In Figure 2, it shows the

kinematic scheme of MRINSPECT 1. The robot has six-slider crank mechanisms and each of them is assembled at  $120^\circ$  from each other. Each of the cranks has a driving wheel which is operated by a DC motor and belt transmission. To simulate the mechanisms with equivalent forces, the robot is designed as the springs and this structure will allow the robot to move within horizontal or vertical pipes.

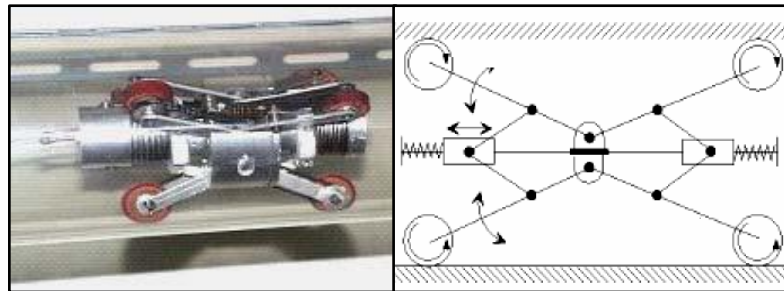


Figure 2 MRINSPECT in pipe robot (a) and its basic mechanism (b)

Even though this design is made to adapt the robot to function inside the pipes, it does not ensure the workability for different pipe diameters. To overcome, there is another design and mechanism which can assure the adaptability of the robots to different pipe diameters. This design will use modified pantograph <sup>[1]</sup>. The structure of this mechanism is shown in Fig 3. The mechanisms allow the robot to move along the radial direction. This feature is very essential to the design of the robot because as the robot passes over any impediments, there will be no distortion forces present. Linear actuators with two position sensors are used in order to manipulate the pushing force over the inner surface of the pipe.

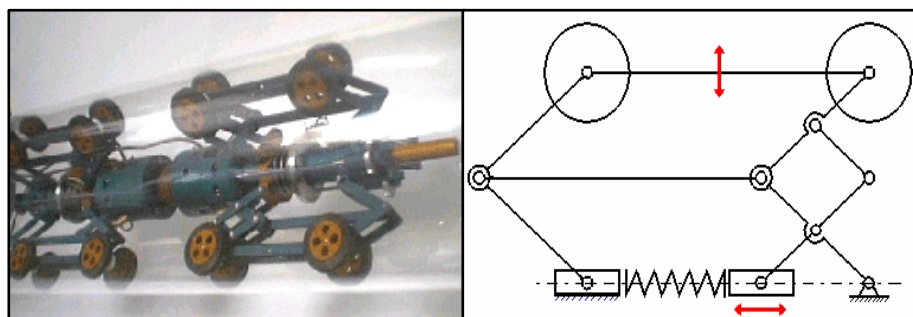


Figure 3 MRINSPECT II (a) and its corresponding mechanism (b)

Figure 4 shows another mechanism in which it allows to adapt its structures to the pipes' diameter. This mechanism will also help to assure the movement and direction of the robot when it passes through elbows and T junctions <sup>[1]</sup>.

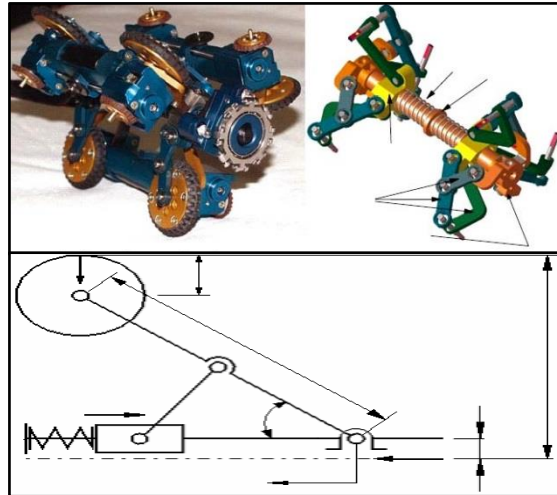


Figure 4 MRINSPECT IV (a) and its corresponding mechanism (b)

In a technical paper presented by O.Tatar, D. Mandru, and I. Ardelean, they have developed a prototype of an in-pipe mini robot. The robot, which consists of three linkages mechanisms which are symmetrically disposed along the longitudinal axis of the robot, are driven by three DC motors. The mechanism and design of the robot is shown in Figure 5. The components of the robot are -helical spring 2-translation element 3-actuator support 4-worm wheel 5-worm gear 6-actuator 7-central axis 8-link 9-wheel.

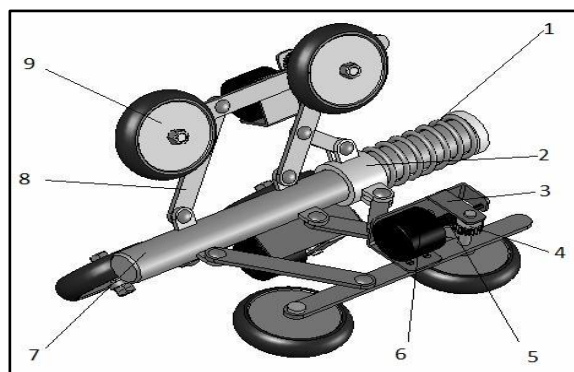


Figure 5 The 3D model of components of minirobot



Even though these types of robots have no limitations on the diameter of the pipe they can function, their operations can only be performed in horizontal or nearly horizontal with limited inclination of pipes only <sup>[11]</sup>. This is due to the constraints on the inclination maximum of the pipe that they can navigate.

#### 2.1.4 Wheeled-type Design with Tilted Wheels

In the wheeled-type designs, the wheels are located in such they will move along or parallel to the pipes. However, another design has been made, with less or more complicated kinematical structures, depending on the diameter adaptability and turning capability <sup>[2]</sup>. The design is the result from an effort to reduce the electrochemical complexity by using only a single actuator in order to achieve higher flexibility along the pipes.

The robot consists of two main parts, a rotor and a stator and they are connected by an active joint including DC motor. To allow the motion parallel to the pipe axis, a set of wheels is installed to the stator and on the rotor, another set of wheels is installed but this set of wheels is tilted with a small angle with respect to the plane perpendicular to the tube axis, as shown in Figure 7.

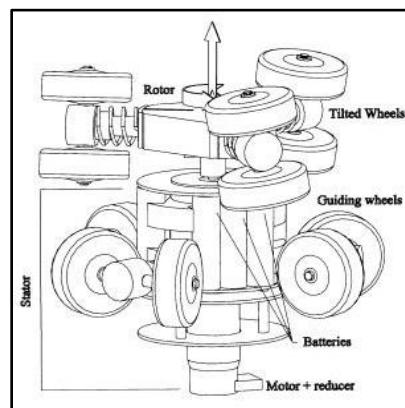


Figure 8 Robot architecture. Two body architecture

In this way, the stator will only be limited to move along the pipe axis while the rotor can only move along helical trajectories, and the axial motion is generated by the rotation of the rotor with respect to the stator. The relation between the axial velocity  $v$  of the robot and the rotation velocity  $w$  is given by

$$v = \omega.R.tg\alpha \quad (3)$$

where  $R$  is the radius of the pipe and  $\alpha$  is the tilting angle of the wheels of the rotor. To assure that the overturning stability of the robots, the wheels on the stator and the rotor must be located in order as sufficient contact force between the robot and the pipe is essential. This is also important to ensure that the robot is able to adapt to small changes in the pipe diameters and obstacles besides allowing it to travel in curved pipes.

This design of using tilted wheels will be different depending on the diameter of the pipes. For the larger pipe diameter ( $D=170$ ), the robot has to be rigidly connected to the axis of the motor and both of the rotor and the stator, three pairs of wheels are sufficient for stability. For small pipe diameter, curved pipes require more degree of freedom <sup>[2]</sup>. This is due to the linking between the rotor and stator does not stay on the axis of the pipes during turning. To achieve more degree of freedom, a universal joint is provided with some axial backlash along the two axes of joint. Also, to achieve overturning stability the number of wheels on the stator has to be increased to double. On the other hand, smaller diameter robots are made of three bodies which are separated by two universal joints as shown in Figure 8. The first body consists of the rotor with the tilted wheels, the second body consists of the motor and the reducer while the third body consists of the stator with the axial wheel, batteries and telecom.

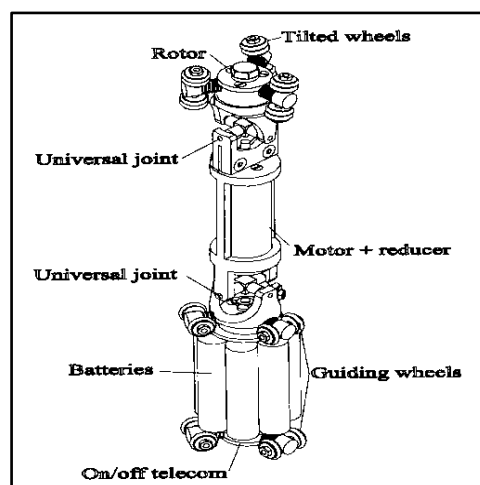


Figure 9 Three body architecture for smaller diameter

Table 1 shows the characteristics of different types of tilted wheels robots; the maximum allowed axial force in addition to the weight when the robot is moving upwards in vertical position.

**Table 1 Main characteristics of the robots**

<b>Robot #</b>	<b>D-170</b>	<b>D-70/1</b>	<b>D-70/2</b>	<b>D-40</b>
Pipe diameter	163-173 mm	68-72 mm	68-72 mm	38-43 mm
Curve radius	>600 mm	>170 mm	>170 mm	>110 mm
Payload	5 N	3N	3 N	1 N
Speed	8 cm/s	10 cm/s	5 cm/s	3 cm/s
Motor power	10 W	6 W	6 W	3.2 W
Gear reduction	33.2:1	19:1	32:1	84:1
Obstacle height	<10 mm	<3 mm	<3 mm	<1 mm
Number of bodies/ universal joints	2 / 0	2 / 1	2 / 1	3 / 2
Weight	1300 g	470 g	480 g	250 g

Even though the design of using wheeled type in-pipe inspection robot is one of the simplest designs, it has its own drawbacks. One of them is the limitations to the shape of the pipe. The wheeled type robots are only suitable to function in a circular cross section of types. If there are any rectangular cross sections, the design has to be modified completely.

### **2.1.5 Inchworm Type Design**

Another design has been developed which is the steerable inchworm type in-pipe inspection robot. This robot, developed by Woongsun Jeon, Jungwan Park, Inho Kim, Yoon Koo Kang, and Hyunseok Yang of Yonsei University Korea has the ability to navigate itself in a wide range of commercial pipes such as vertical, curved, Y and T-branch pipes <sup>[4]</sup>. Their design is different from any other inchworm design which has the limitation in functioning in those conditions. It can also function not only in circular cross section but also in rectangular cross section. The robot is made out of two parts; the first part consists of two clamper modules and the second part consists of one extensor module. The two clamper modules are attached to both ends of the extensor module respectively.

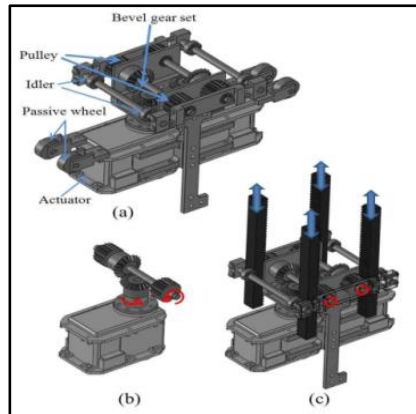


**Figure 10 Extensor module (a) main components. (b) Power transmission (c) Continuum links and its linear motion**

The extensor module, as shown in Figure 10 mainly comprises of a frame, four continuum links which are attached with a timing belt respectively, pulleys, bevel gear sets, passive wheels, and two actuators. The frame is designed in order to decrease its weight. There are two pulleys connected to a shaft and they are driven by with an actuator through a set of bevel gears, as shown in Figure 10. A timing belt is used to create a linear motion of the continuum links by the rotation of the pulleys as illustrated <sup>[4]</sup>.

The clamper modules on the other hand, are divided into two sections; the upper clamper modules and the lower clamper modules. The modules, as shown in Figure 11, consists of four crank-slider mechanisms that are located in array with 90 spacing between each other, and a servo motor, with four cranks connected to it <sup>[4]</sup>. By doing this, when the four cranks are rotated at the same time by using a single servo motor, the rotary motion by the servo motor is transformed to a reciprocating linear motion of sliders along a guide. The advantage of having crank-slider mechanism is it allows the robot to adapt to various pipe diameters and act normal force to an uncertain in-pipe surface.

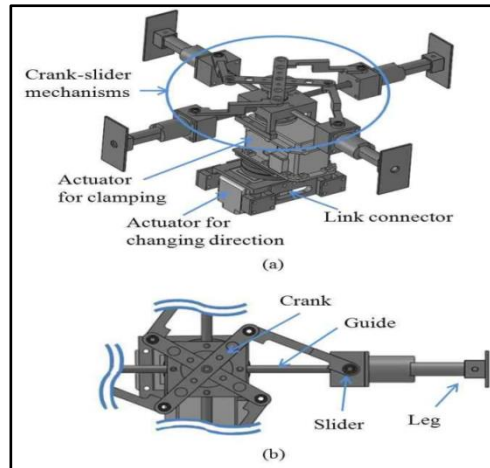


**Figure 11 Upper clamber module. (a) Main components of clamber module. (b) Crank-slider mechanism**

The locomotion of this robot is based on the inchworm locomotion and as mentioned before, it is composed of clamping motions and extension motions. At the start of the locomotion, the lower clamber module will adhere to the inner surface of the pipe, and the robot sets the position at the center of the pipe. Then, the upper clamber module is stroked by the extensor module. After the upper clamber module clamps its legs to the inner surface of the pipe, the lower clamber module will withdraw its legs that were adhered to the pipe and then the extensor module will pull the lower clamp modules.

### 2.1.6 Snake and Legged Robot

The mechanisms of snake and legged robots permit them to move in different type of motions as both of them have many degrees of freedom <sup>[11]</sup>. In spite of having many degrees of freedom, these kinds of robots will result them to require higher numbers of actuators and thus increases its complexity compared to the robots that are using different locomotion types <sup>[11]</sup>. Examples of legged pipe inspection robots can be found in the works of (Neubauer 1994) and (Zagler and Pfeiffer 2003) and are capable of navigating bends and junctions in a pipe. Similarly, snake robots used for pipe inspection can be seen in (Kuwada et al. 2008; Fjerdingen, Liljeback, et al. 2009; Wright et al. 2007). These robots comprise of a number of modules and they are connected together using actuated joints <sup>[11]</sup>.

### 2.1.7 Size of In-pipe Robot

Due to the geometric constraints of the pipeline configurations, the robot has to be designed in such a way that it will satisfy the constraints. For example in an elbow, the robot can be modeled as cylinder relations can be derived among the elbow's diameter, the curvature and the size of the robot <sup>[7]</sup>. The most unfavorable position a robot can be is when it is oriented with 45° as shown in the figure

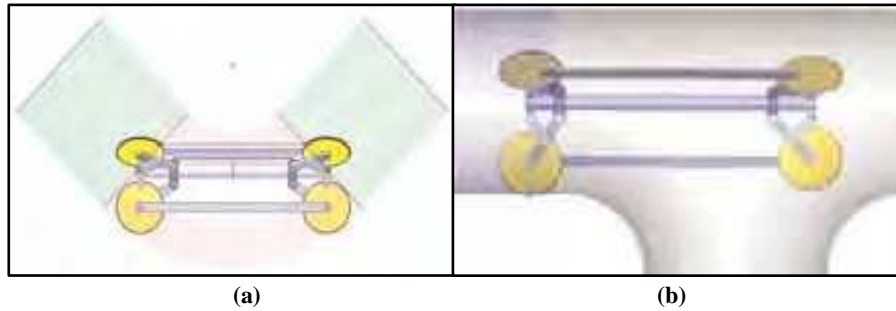


Figure 12 Size of the robot (a) Negotiating with the elbow (b) Negotiating with the branch

There are two situations that have been considered upon determining the length of the robot;

- i. The diameter of the robot is relatively smaller than the height  $h$ , and both ends of the robot,  $p'$  and  $p''$  are located on the same region of the pipeline <sup>[7]</sup>.
- ii. Both ends of the robot are involved in the elbow.

For the case of (a),

$$0 < D_r \leq \left\{ \left( r_c + \frac{d}{2} \right) \sin 45^\circ - \left( r_c - \frac{d}{2} \right) \right\} \quad (4)$$

The length of the robot is given by;

$$L_r = 2\sqrt{2} \left\{ \frac{d}{2} + r_c - \frac{d}{2} + D_r \right\} \cos 45^\circ \quad (5)$$

In the case of (b), the range of  $D_r$  is obtained by

$$\left\{ \left( r_c + \frac{d}{2} \right) \sin 45^\circ - \left( r_c - \frac{d}{2} \right) \right\} < D_r < D \quad (6)$$

Thus the length of the robot  $L_r$  will become

$$L_r = 2 \sqrt{\left( r_c + \frac{d}{2} \right)^2 - \left( r_c - \frac{d}{2} + D_r \right)^2} \quad (7)$$

And it is rewritten by

$$0 < L_r < \frac{3}{2} \sqrt{2D} \quad (8)$$

## Summary

To summarize, there is no ideal mechanism for pipe inspection robot that can maximize all the requirements that are needed for pipe-inspection robot like stability, maneuverability and controllability. Each design will have constraints on it and it can be determined on the applications of the design.

## Chapter 3: Methodology

### 3.1 Project Activity

#### 3.1.1 Literature Review

The research for designs of mechanisms for in-pipe inspection robot is done by reading journals and articles that are obtained from the internet. This is vital because there are numbers of mechanisms that have been developed and each of them has its own advantages and disadvantages. The journals are read and cross referencing is done to compare and contrast the different mechanisms of the robot. The research is essential in as it can be set as an initial datum or as a reference to be improved.

The design for the robot will be based on a design called MRINSPECT III (*Multifunctional Robotic crawler for Inpipe inspection*) that applies the pantograph mechanism with a sliding base that allows the natural folding and unfolding of the robot's legs. The wheeled leg mechanisms of the design are simulated but using different parameters based on the objective of this project.

#### 3.1.2 Design and Modeling

The design is based on a wheeled type robot called *Multifunctional Robotic Crawler for In-pipe Inspection* or MRINSPECT. The robot comes in many series and for this project, the series that will be used as a reference is the MRINSPECT III. The mechanism of movement of the robot will be the guide.

- i. Before designing the robot some parameters have to be met. The parameters are;
  - The maximum height and width of the robot must be 10 inches (250mm) and the minimum height of the robot must be 6 inches (150mm).

- The locomotion of the robot must be in wheeled-type design in which the slider crank is placed  $120^\circ$  from each other.
  - The robot is functioning in a horizontal or near horizontal pipe.
  - The robot is powered by an electric motor and thus no combustion engine is used.
- ii. The dimension of the robot is done by calculations and with the following assumptions.
- Radius of the wheel =  $25\text{mm}^{[1]}$
  - Radius of the link =  $5\text{mm}$
  - Radius of the central shaft =  $10\text{mm}$
  - Allowance =  $4\text{mm}$
  - Initial folding angle of the link =  $45^\circ$
- iii. After the design is selected, it is modeled in details. The design must be modeled in a way that it is realistic and can be fabricated. The modeling activity is done by using modeling software AutoCAD 2007.

### 3.1.3 Simulation

- i. Simulation is conducted by using ADAMS View 2005 to observe the robot's movement when it travels through large pipe diameter (10 inches) and small diameter (6 inches).
- ii. The simulation is done by modeling one of the legs of the robot according to the dimensions calculated.
- iii. The wheel is set to be rubber with density,  $\rho = 1.1 \times 10^{-6} \text{ kg/mm}^3$ , Young's Modulus =  $1 \times 10^4 \text{ newton/mm}^2$ , Poisson's ratio = 0.5.

- iv. The surface of the pipe is set to be steel with density,  $\rho = 7.801 \times 10^{-6}$  kg/mm<sup>3</sup>, Young's Modulus =  $2.07 \times 10^5$  newton/mm<sup>2</sup> and Poisson's ratio = 0.29.
- v. The static coefficient of friction between rubber and steel is set to be 0.7 and the dynamic coefficient between rubber and steel is set to be 1.
- vi. The speed of motor is set to be 25000\*d / time.
- vii. The simulation is done with step size 0.001 and end time 50.
- viii. After the simulation is complete, the results of force, velocity, spring deformation, and torque is observed and analyzed.

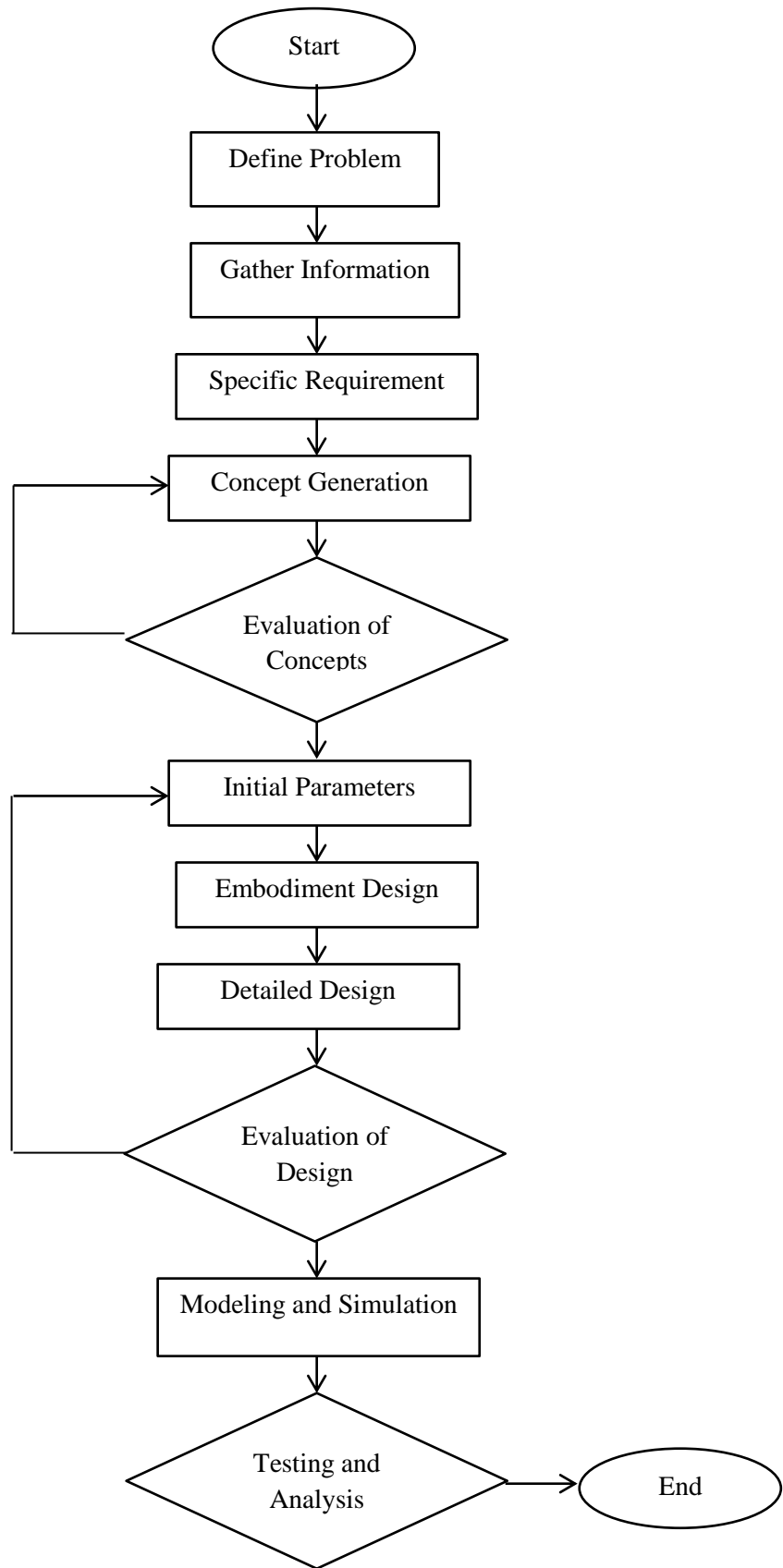


**Figure 13 Process flow of the project**

### 3.2 Gantt Chart

**Table 2 Gantt Chart For Final Year Project I**

No	Details/week	1	2	3	4	5	6	7	8	9	10	11	12	13	14
1	Title Selection	■	■												
2	Literature Review			■	■	■									
3	Design Concept						■	■							
4	Proof Working								■						
5	Design Concept Evaluation									■	■				
6	Detail Design											■	■		
7	CAD Modeling													■	■

■ - Progress

**Table 3 Final Year Project I Milestones**

No	Details/week	1	2	3	4	5	6	7	8	9	10	11	12	13	14
1	Completion of title Selection		●												
2	Completion of literature Review					●									
3	Completion of design Concept							●							
4	Completion of proof Working								●						
5	Design Concept Evaluation										●				
6	Detail Design												●		
7	CAD Modeling														●

● - Milestones

**Table 4 Gantt Chart for Final Year Project II**

No	Details/week	1	2	3	4	5	6	7	8	9	10	11	12	13	14	15
1	CAD Design	█	█													
2	Simulation			█	█											
3	Analysis					█	█	█								
4	Progress Report submission								█							
5	Final Report Preparation									█	█					
6	Pre-SEDEX											█				
7	Draft Report Submission												█	█	█	
8	Draft Technical Paper Submission													█	█	
9	Oral Presentation														█	
10	Project Dissertation															█

**Table 5 Final Year Project II Milestones**

No	Details/week	1	2	3	4	5	6	7	8	9	10	11	12	13	14	15
1	Completion of CAD Design		●													
2	Completion of simulation				●											
3	Completion of analysis							●								
4	Completion of progress report submission								●							
5	Completion of final report preparation										●					
6	Completion of Pre-SEDEX											●				
7	Completion of draft report submission														●	
8	Completion of draft technical paper submission														●	
9	Completion of oral presentation														●	
10	Completion of project dissertation															●

## Chapter 4: Results and Discussion

### 4.1 Robot's Designs and Development

Some specifications have to be met in order to design the robot;

- The maximum height and width of the robot must be 10 inches (250mm) and the minimum height of the robot must be 6 inches (150mm).
- The locomotion of the robot must be in wheeled-type design in which the slider crank is placed 120° from each other.
- The robot is functioning in a horizontal or near horizontal pipe.
- The robot is powered by an electric motor and thus no combustion engine is used.

#### 4.1.1 Robot's Mechanism

For this project, the mechanism of the robot will be designed based on MRINSPECT III and MRINSPECT IV. The mechanism of the robot uses pantograph and a sliding base and it has 6 slider crank mechanisms which are arranged 120° from each other. The purpose of this mechanism is to allow the wheels to move in radial direction <sup>[1]</sup>.

The figure shows the kinematic diagram of MRINSPECT III wheeled leg mechanism which uses a pantograph with a sliding base that allows the folding and unfolding of the legs <sup>[7]</sup>.

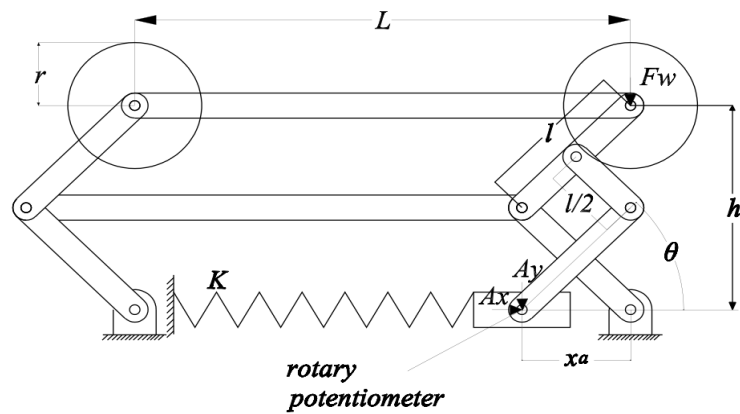


Figure 14 Kinematic Diagram of MRINSPECT III

With this mechanism when the robot encounters any obstacles in the pipe, the wheels will contract or expand along the radial direction. This will also be advantageous when the robot has to function in different pipe diameters. In this diagram;

$l$  = length of the link

$\theta$  = folding angle of the link measured by the rotary potentiometer

$K$  = spring constant

$h$  = distance of the center of the wheel from the base

$F_x$  = wall pressing force

$A_x, A_y$  = forces acting on the link by the spring

$x$  = displacement of the sliding base

Using the figure shown basic equations can be derived necessary for optimizing the wall pressing forces.

#### 4.1.2 General Dimension of the Robot

Some dimension requirements have to be met before designing the robot. For this case, the robot must function in a pipe diameter ranging from 6 inches to 10 inches. So the requirements for the robot will be;

- The maximum height of the robot is 10 inches (250mm)
- The maximum width of the robot is 10 inches (250mm)
- The minimum height of the robot is 6 inches (150mm)
- The minimum width of the robot is 6 inches (150mm)
- The length must be in a way that it can fit while making a turn in the smallest pipe diameter (150mm)

Before those requirements are met, there are some considerations that need to be satisfied. It is known that the design of the robot is based on MRINSPECT III which has a sliding base mechanism. So the central axis's dimension has to be taken into considerations as well as the translational element which is the sliding base.

The maximum height of the robot measured from the center is 125mm. A few parameters have to be considered and predefined before determining the maximum height,  $h$ . From the figure, they are;

- Radius of the wheel = 25mm<sup>[1]</sup>
- Radius of the link = 5mm
- Radius of the central shaft = 10mm
- Allowance = 4mm
- Initial folding angle of the link = 45°

By using these assumptions,  $h_{max}$  can be found with;

$$h_{max} = 125 \text{ mm} - 25\text{mm} - 5\text{mm} - 4\text{mm} - 10\text{mm}$$

$$h_{max} = \mathbf{81\text{mm}}$$

From this, the displacement of the sliding base,  $x$  can be found using the following equation;

$$h_{max} = 2x \tan \theta$$

$$81\text{mm} = 2x \tan 45$$

$$x = 40.5mm$$

The value of  $x$  can be used to determine the length of the link,  $l$  by the following expression:

$$h = 2\sqrt{l^2 - x^2}$$

$$81 = 2\sqrt{l^2 - 40.5^2}$$

$$l = 57.28 mm$$

From the diagram,  $l$  is the length of DE and the length of link DC and BA is the same which is 57.28 mm and the length of BG will be  $57.28/2 = 28.64 mm$ .

The length of the robot is determined by considering two conditions; the height of the robot is relatively bigger than the diameter of the robot with both ends of the robot are located in the region of the straight pipeline and both ends of the robot are included in the elbow<sup>[7]</sup>. The length of the robot can be determined by the following expression;

$$L_r = 3(\sqrt{2} - 1)D$$

The diameter  $D$  is set to be 150 mm because it is the minimum diameter that the robot can pass through.

$$L_r = 3(\sqrt{2} - 1)150mm$$

$$L_r = 186.4mm$$

The length is then set to be **185 mm**. The figures below shows the side view of one of the legs of the robot and the main body frame modeled using AutoCAD based on the calculation that has been done previously.

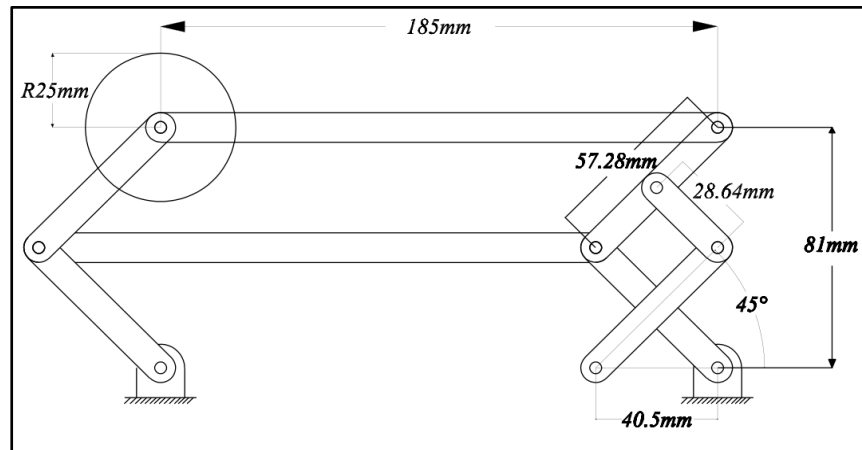


Figure 15 Side View of One of the Legs

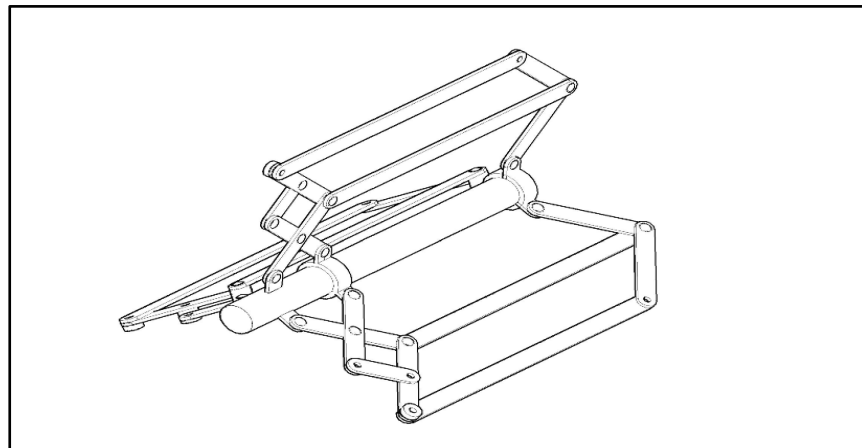


Figure 16 CAD model of the main body frame

### 4.1.3 Spring Design

Spring in this mechanism plays a vital role as it provides reflective forces that support the moving base of the pantograph. The spring will then produce the wall pressing forces. Thus the wall pressing forces can easily be predefined by altering the spring constant and initial condition. The spring is also important as it ensures that wall pressing force is sufficient to keep the wheels adhered to the inner surface of the pipe and thus keeping it from falling due to gravity.

Some parameters are predefined for the spring. They are;

- Number of coils = 20 turns
- Number of active coils,  $n_a = 20 - 2 = 18$
- Outer diameter ,  $OD = 25$  mm
- Diameter of spring,  $d = 2.5$  mm
- The spring is closed and had ground ends.
- The spring is stainless steel, AISI type 302
- Free length = 134.4969 mm

Mean diameter,  $D_m$

$$D_m = OD - d$$

$$D_m = 25\text{mm} - 2.5\text{mm}$$

$$D_m = \mathbf{22.5\text{mm}}$$

Pitch, closed & ground,  $p$

$$p = \frac{FL - 2d}{n_a}$$

$$p = \frac{134.4969\text{ mm} - 2(2.5\text{ mm})}{18}$$

$$p = \mathbf{7.19}$$

The diameter of a compression spring will increase when compressed. This increase is a function of the pitch. The expansion of outer diameter, OD can be expressed by the following expression;

$$OD_{\text{expansion}} = \left[ \sqrt{D_m^2 + \frac{p^2 - d^2}{\pi^2}} + d \right] - OD$$

$$OD_{\text{expansion}} = \left[ \sqrt{22.5^2 + \frac{7.19^2 - 2.5^2}{\pi^2}} + 2.5 \right] - 25\text{mm}$$

$$OD_{expansion} = \mathbf{0.10209\ mm}$$

The spring constant is calculated by using the following expression;

$$k = \frac{Gd^4}{8D^3.n_a}$$

Where  $G$  is found from the material's elastic modulus  $E$  and Poisson's ratio  $n$

$$G = \frac{E}{2(1 + \nu)}$$

$$G = \frac{193Gpa}{2(1 + 0.30)}$$

$$G = \mathbf{74.231\ Gpa}$$

Thus  $k$ ;

$$k = \frac{Gd^4}{8D^3.n_a}$$

$$k = \frac{74.231(2.5 \times 10^{-3})^4}{8(22.5 \times 10^{-3})^3.18}$$

$$k = \mathbf{1770\ N/m}$$

Figure 17 below shows the spring modeled using AutoCAD and its dimension while Figure 18 shows the spring installed to the main body frame.

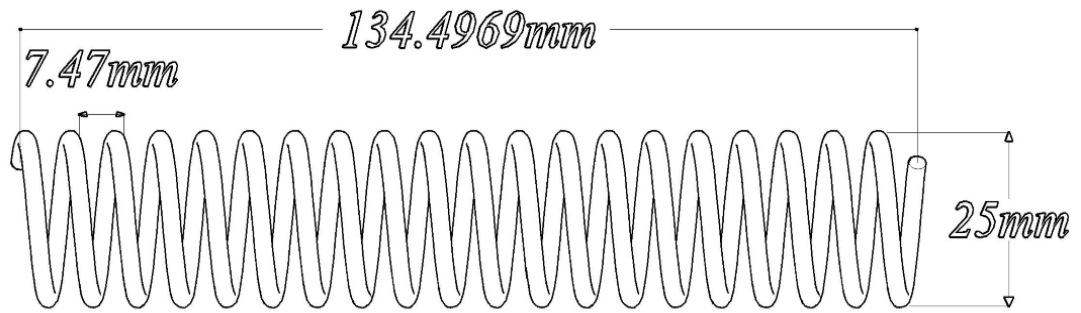


Figure 17 Spring Design

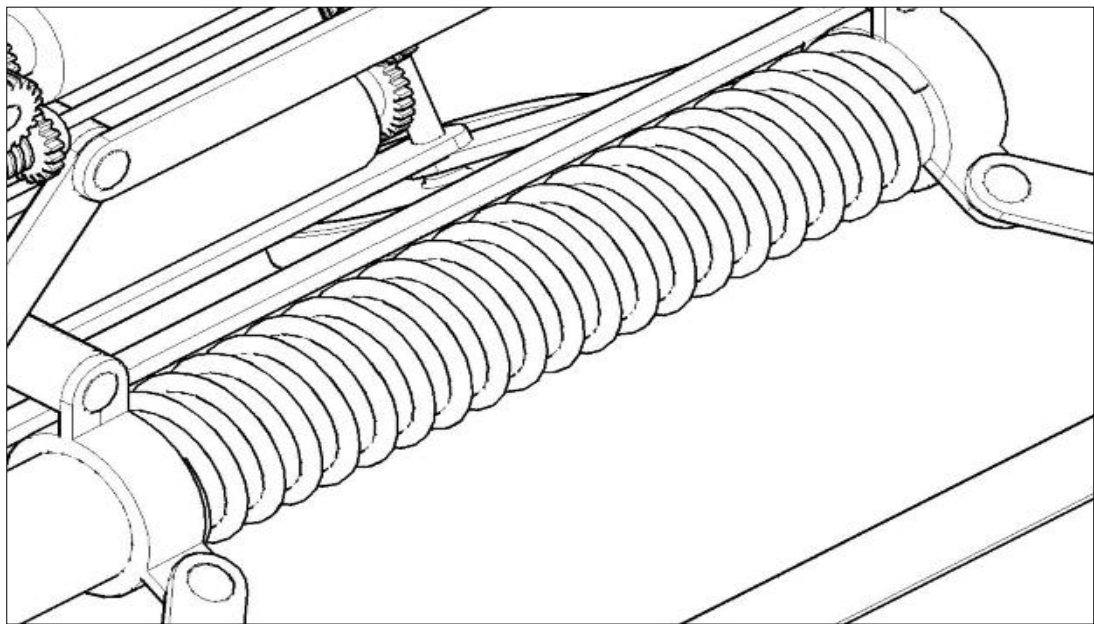


Figure 18 Spring attachment to the main body frame

#### 4.1.4 Driving Mechanism

This robot is driven by three driving modules which are connected at both front and rear wheels of the robot and they are placed circumferentially  $120^\circ$  apart from each other. The driving modules consisting of a geared DC motor, encoder, gears, and two wheels as shown in the figure. Both of the wheels are driven by a single DC motor and the power is transmitted through a set of gears; worm gears and

spur gears and the direction of motion of the rotating units are denoted as  $\omega$  as shown in the figure.

The driving module of this robot is designed to be easily taken apart from them body frame and thus maintenance can be conveniently done. Since the driving modules are independently, the modules will magnify traction forces that ensure enough traction and adhesion forces of the wheels to the surface of the pipes on moving upwards in the vertical pipelines.

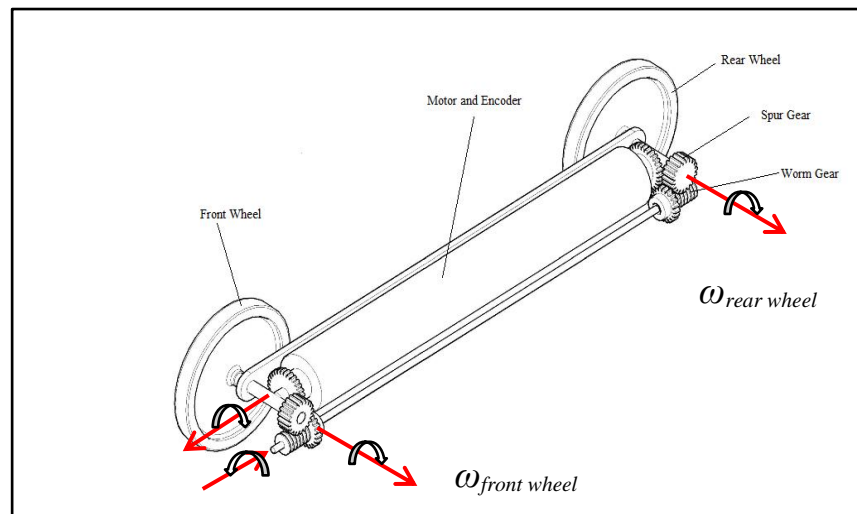


**Figure 19 Driving Modules with sets of gears**

The followings are the specifications of the motor (Maxon, 4.5W) that suits the functionality of the robot inside the pipes;

- Diameter,  $\phi = 26\text{ mm}$
- Power,  $P = 4.5\text{ W}$
- Speed,  $n = 3890\text{ rpm}$
- Torque,  $T = 4.53\text{ mNm}$

## 4.2 Design Models

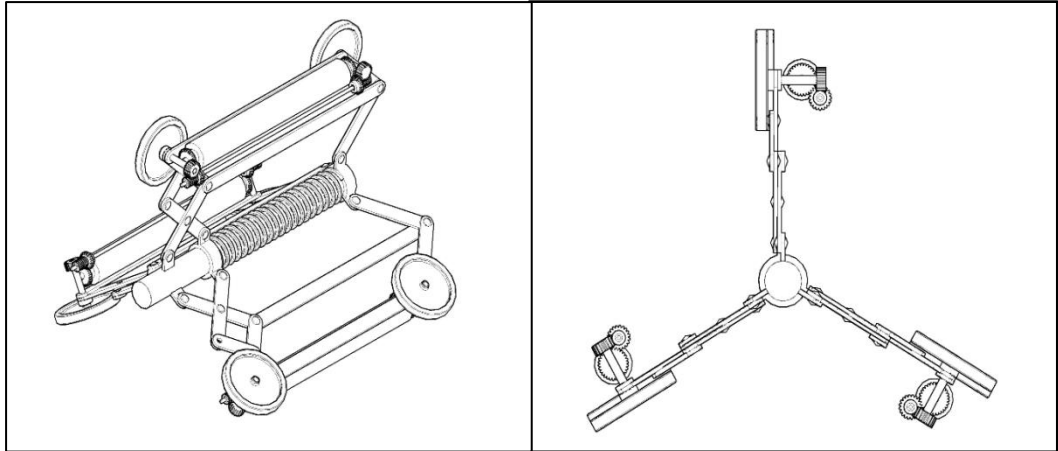


Figure 20 Robot's model in 10 inches diameter

Figure 20 shows the 3 Dimensional model of the robot when it is functioning in maximum pipe diameter 10" while Figure 21 shows the three-dimensional model of the robot functioning in minimum pipe diameter 6".

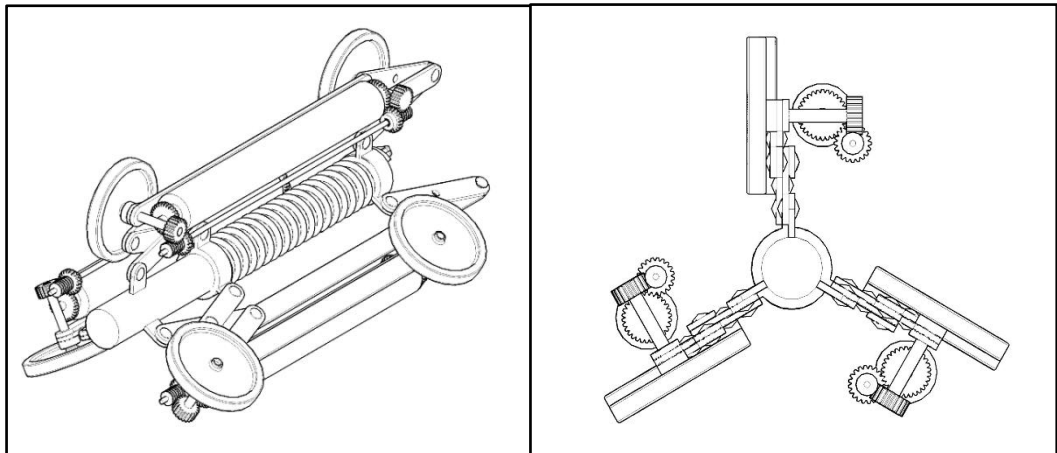


Figure 21 Robot's model in 6 inches diameter

## 4.3 Simulation

### 4.3.1 Spring Deformation and Forces

The graph below shows the deformation of spring as the robot travels from pipe diameter of 10 inches to 6 inches. As can be seen from the graph, the deformation is almost 0 when it travels through 10 inches diameter and the increases as it travels through 6 inches of diameter.

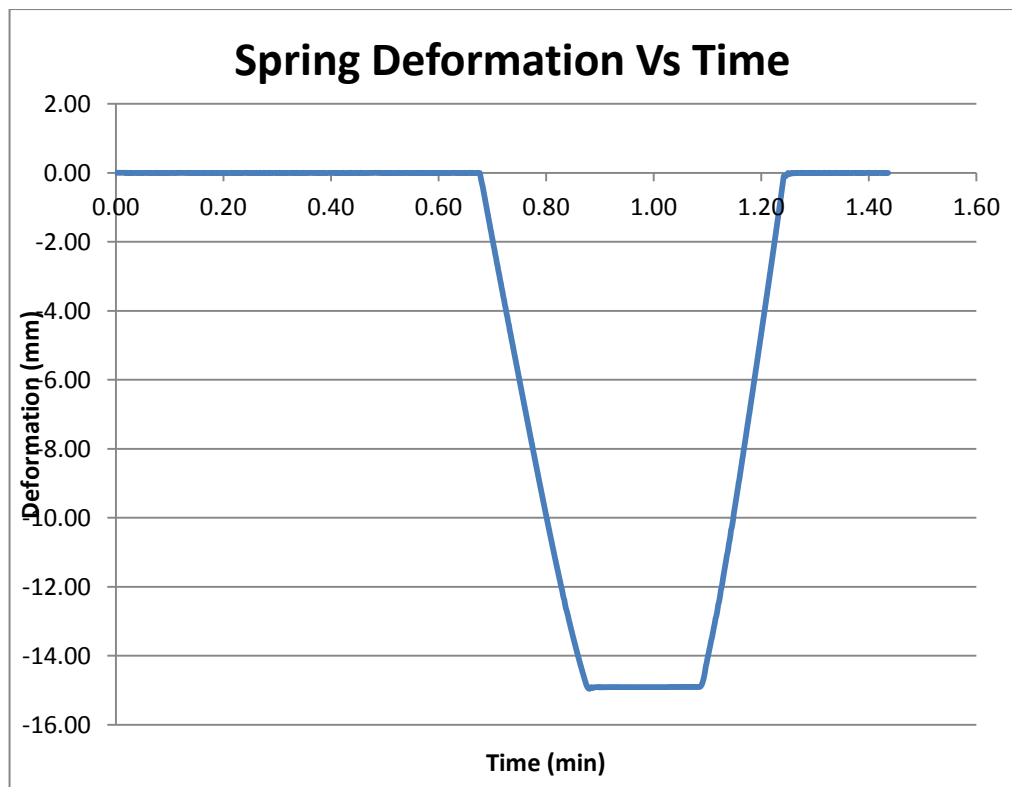


Figure 22 Spring deformation VS Time

The deformation of spring can be used to determine the forces acting on the link by the spring. Since one end of the spring is attached to the sliding base so the deformation of spring will be equal to the displacement of the sliding base. The forces acting on the link by the spring can be determined by the following expression

$$F = -k(\Delta x)$$

Where;

$\Delta x$  = displacement of sliding base (mm)

$k$  = spring constant (N/mm)

when these forces are plotted into a graph, the following is obtained,

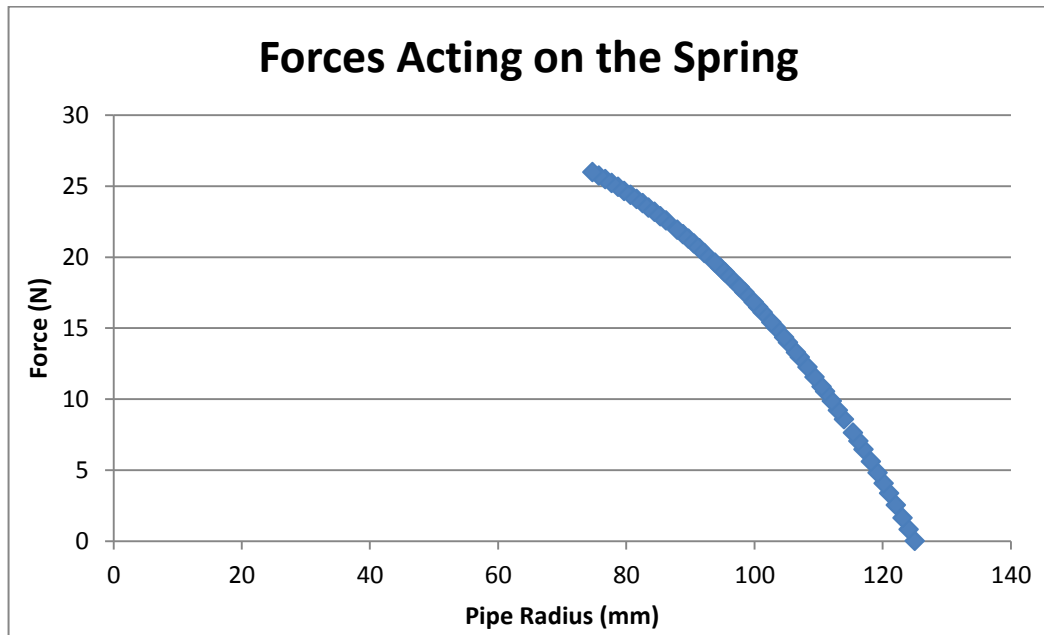


Figure 23 Forces against Pipe Radius

From the graph shown, it can be observed from the simulation using ADAMSView2005, the forces acting on the spring increase with the decrease in diameters of the pipe. Following Hooke's Law;

$$F = -k(\Delta x)$$

When the robot is at the maximum diameter (10 inches), there is little deflection in the spring,  $\Delta x = -0.000000019505\text{mm}$  and the force will be very little compared to the force exerted when the deflection is large.

$$F = -1.770\text{N/mm}(-\Delta 0.000000019505\text{mm})$$

$$F = 3.45 \times 10^{-8} \text{ Newton}$$

When the robot is at minimum diameter (6 inches) the deflection of the spring is 14.7 mm. Again, following Hooke's Law,

$$F = -1770\text{N/m}(-\Delta 0.0147\text{m})$$

$$F = 27 \text{ Newton}$$

With this value of forces acting on the link is determined; the value of wall pressing forces can now be obtained with the following expression;

$$F = \frac{2F_w x}{\sqrt{l^2 - x^2}}$$

Where;

$F$  = forces acting on the link by the spring

$F_w$  = wall pressing force

$l$  = length of the link

$x$  = displacement of the sliding base

$l$  has been determined before to be 57.28 mm and  $x = 40.5$  mm and thus the wall pressing force will be

$$F = \frac{2F_w x}{\sqrt{l^2 - x^2}}$$

$$27 = \frac{2F_w(40.5)}{\sqrt{57.28^2 - 40.5^2}}$$

$$F_w = 13.5 \text{ Newton}$$

### 4.3.2 Forces Acting on Each Joint

As shown in the figure below, there the forces acting on each joint during simulation is observed and analyzed.

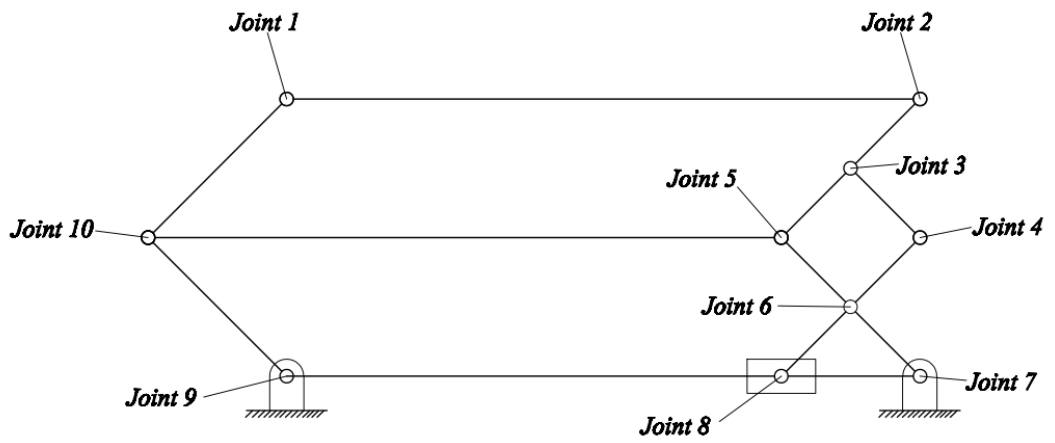
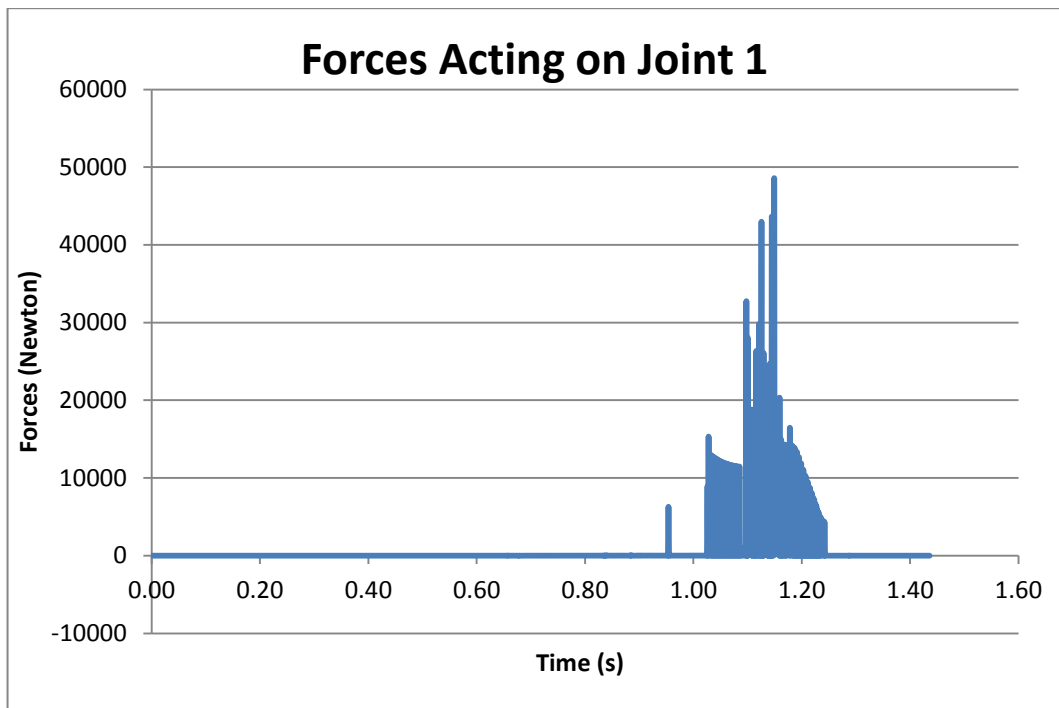
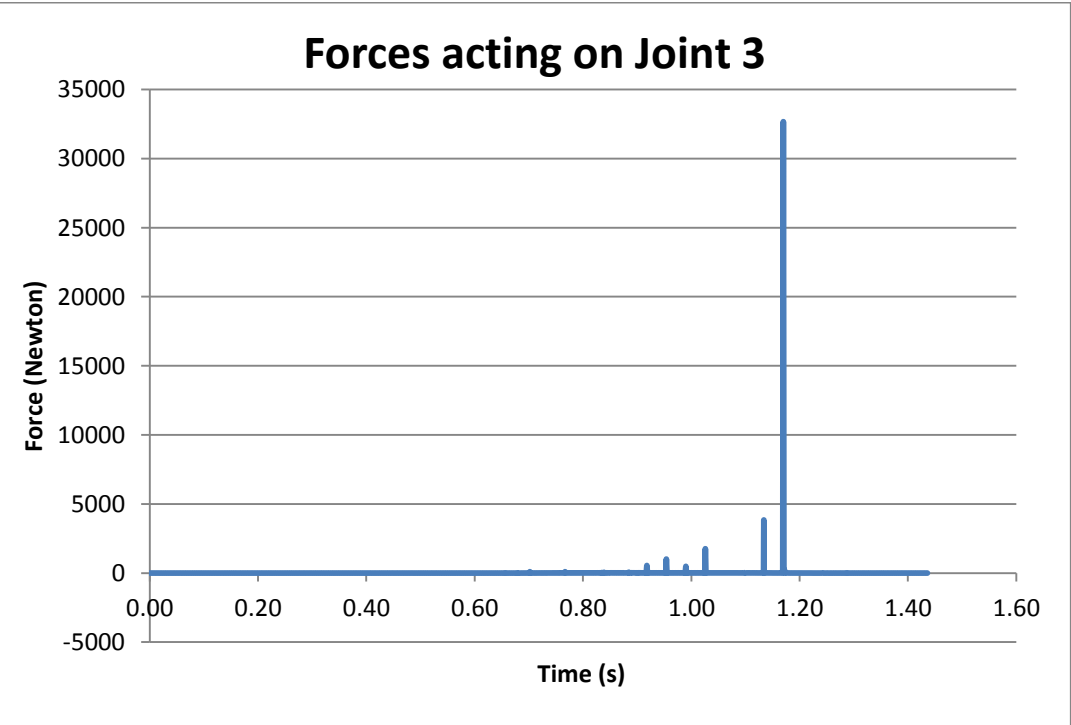
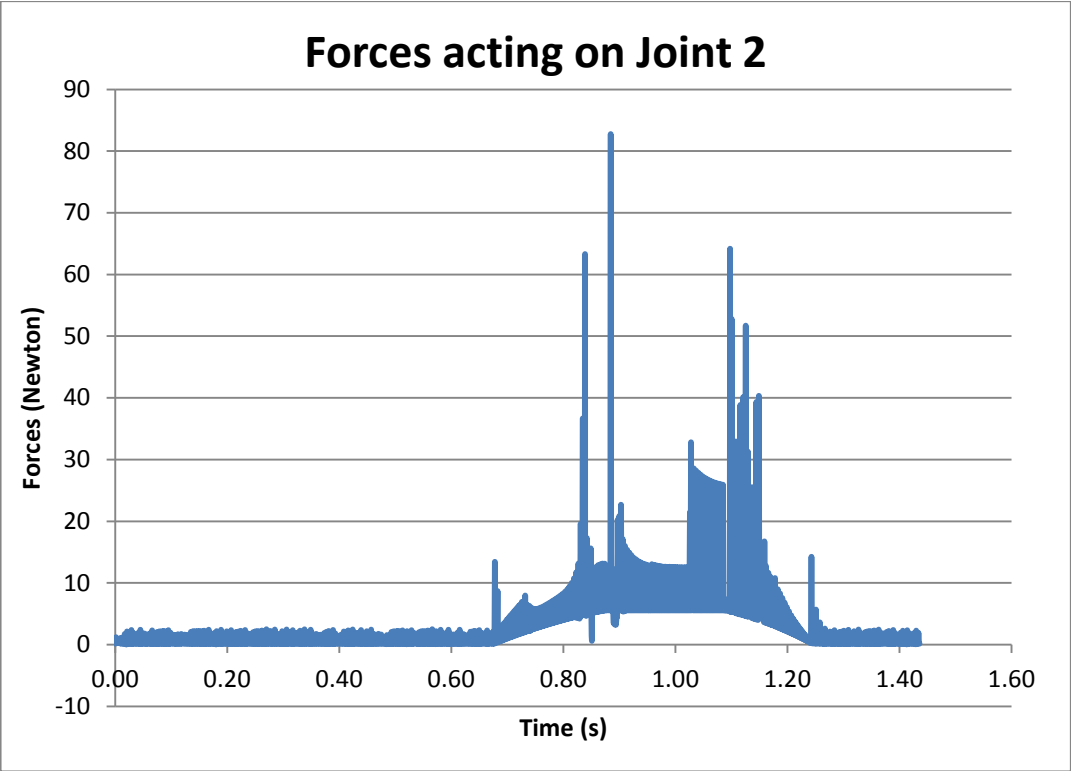
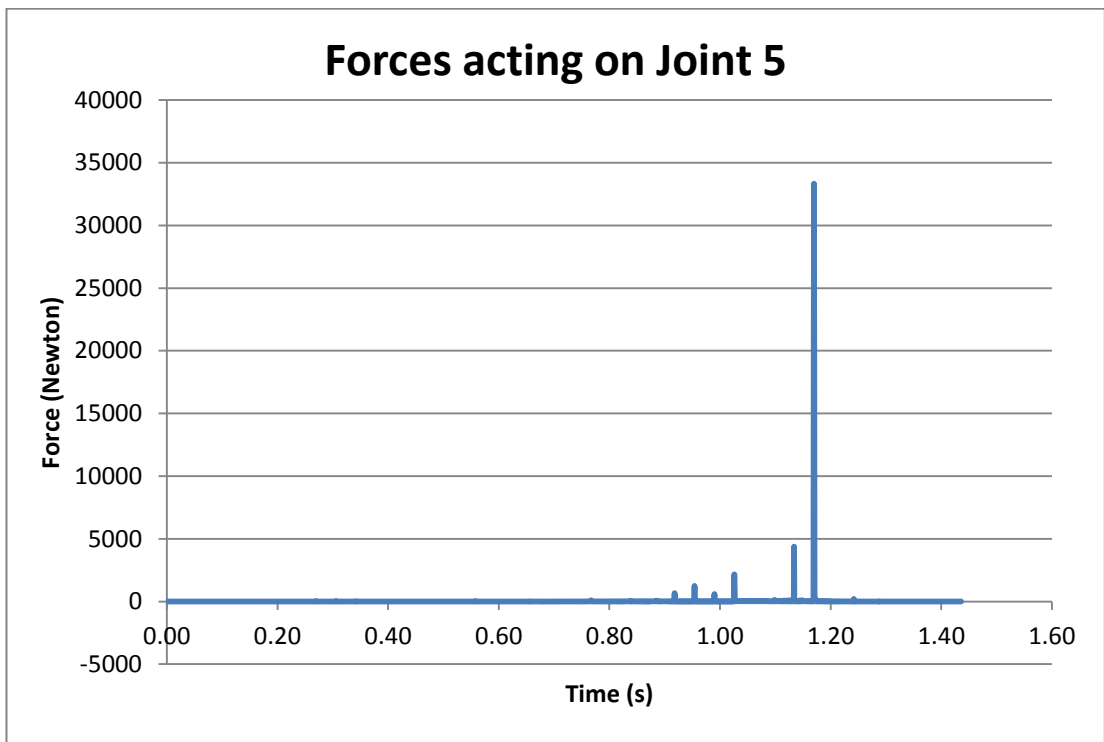
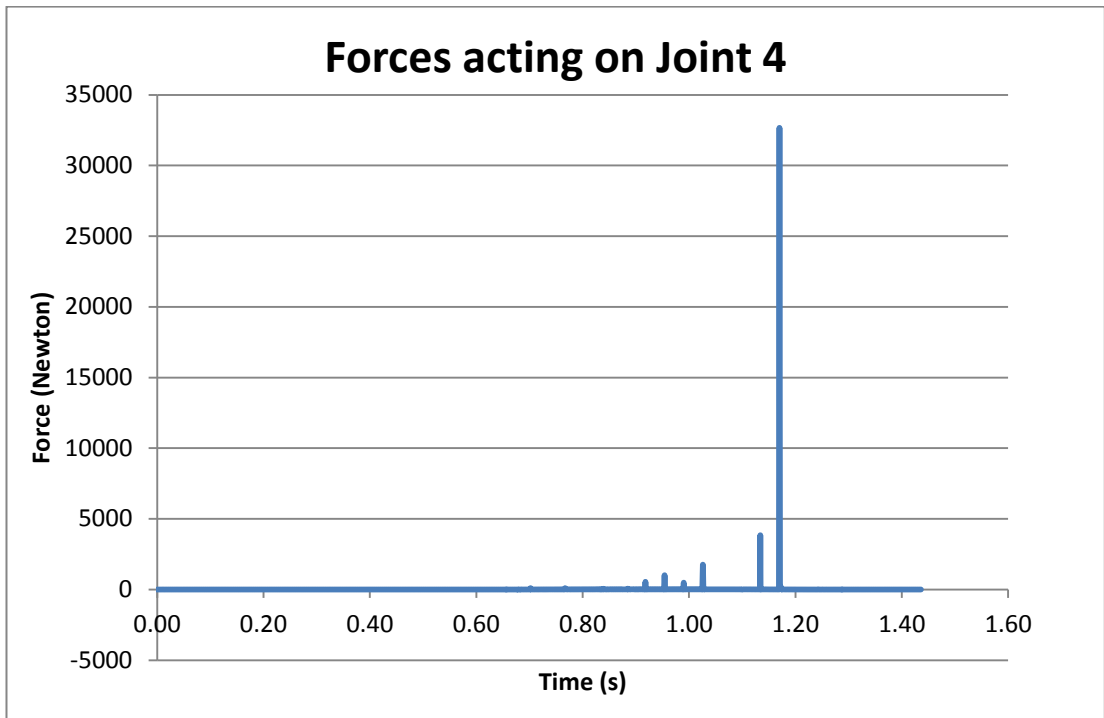
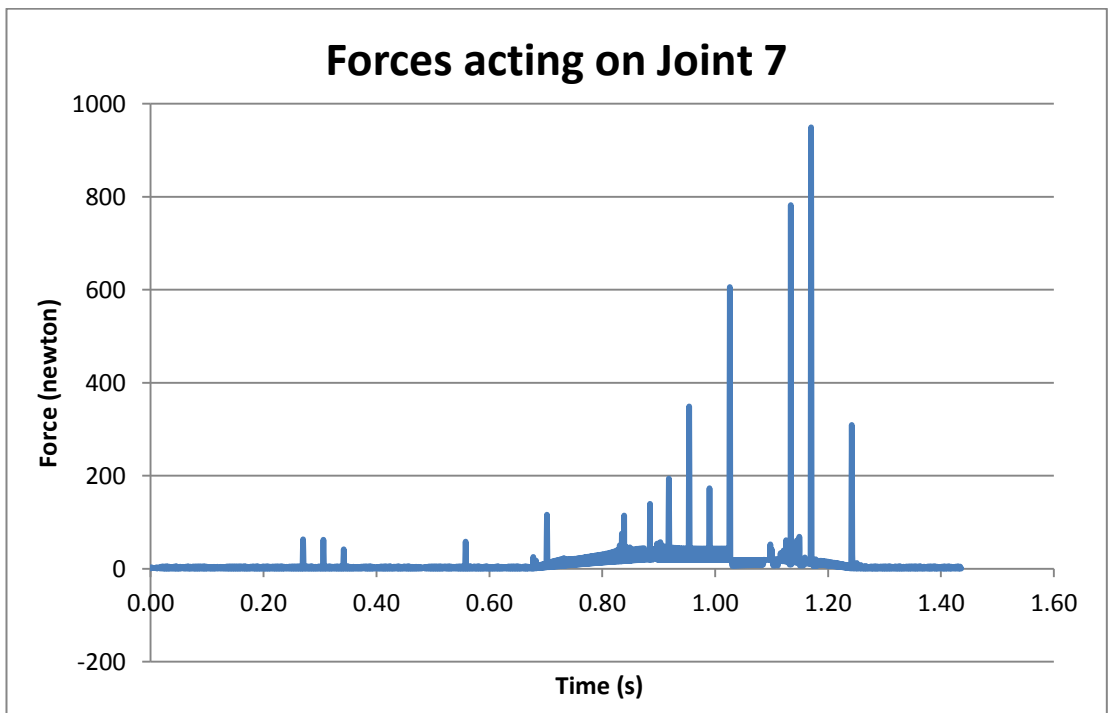
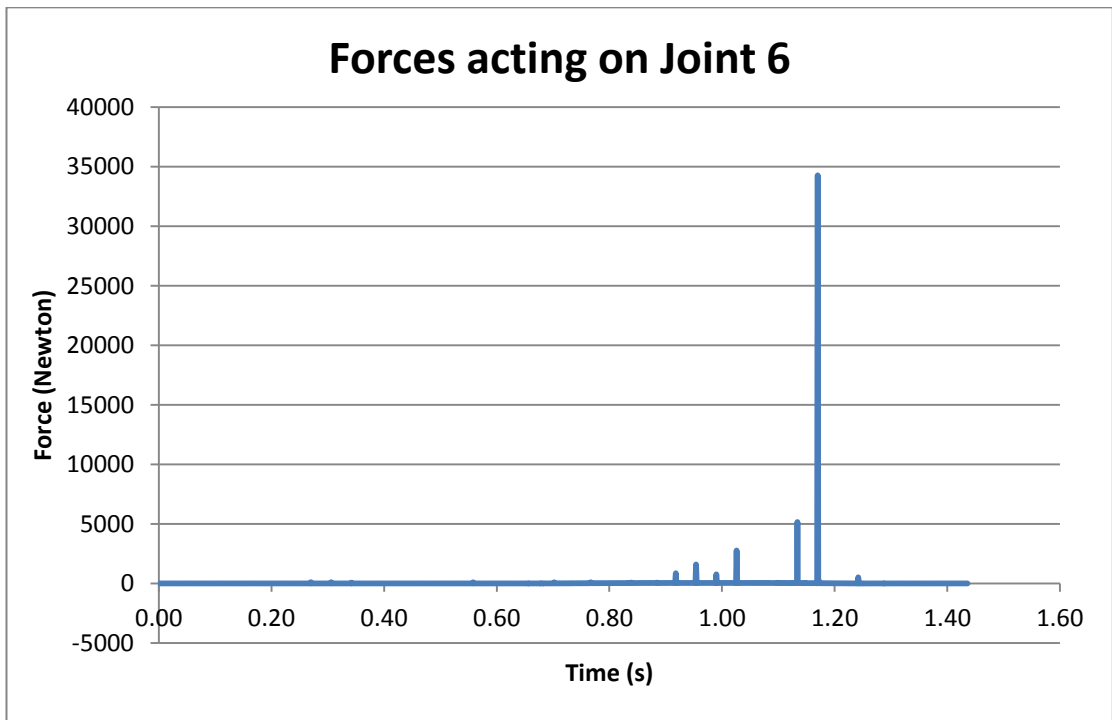


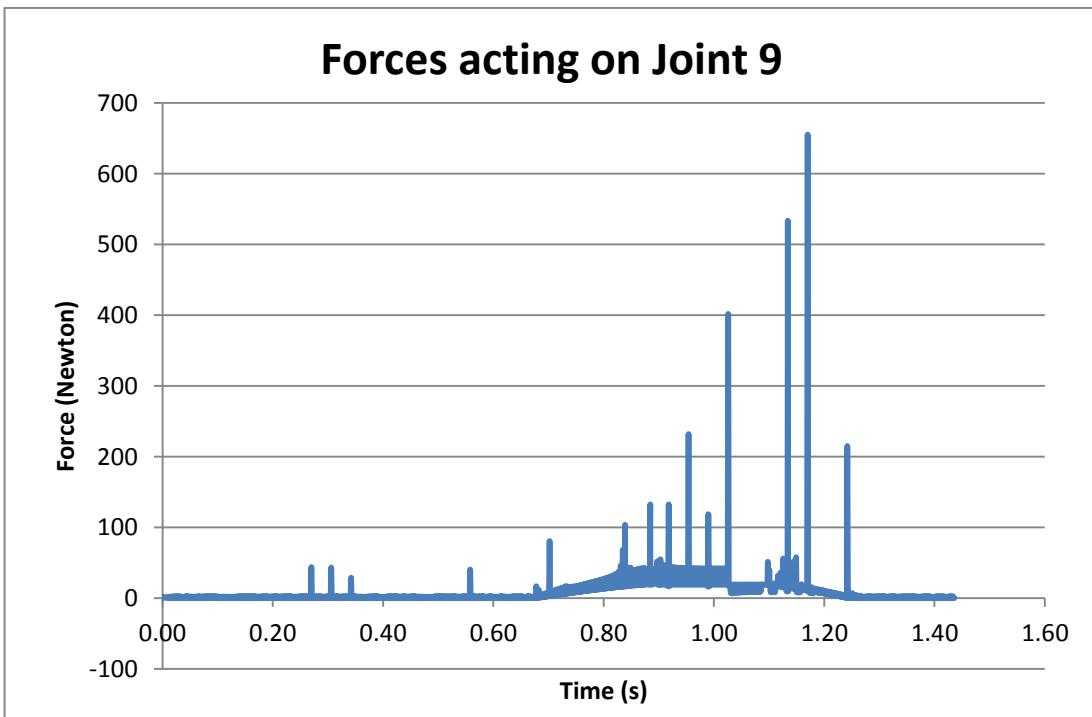
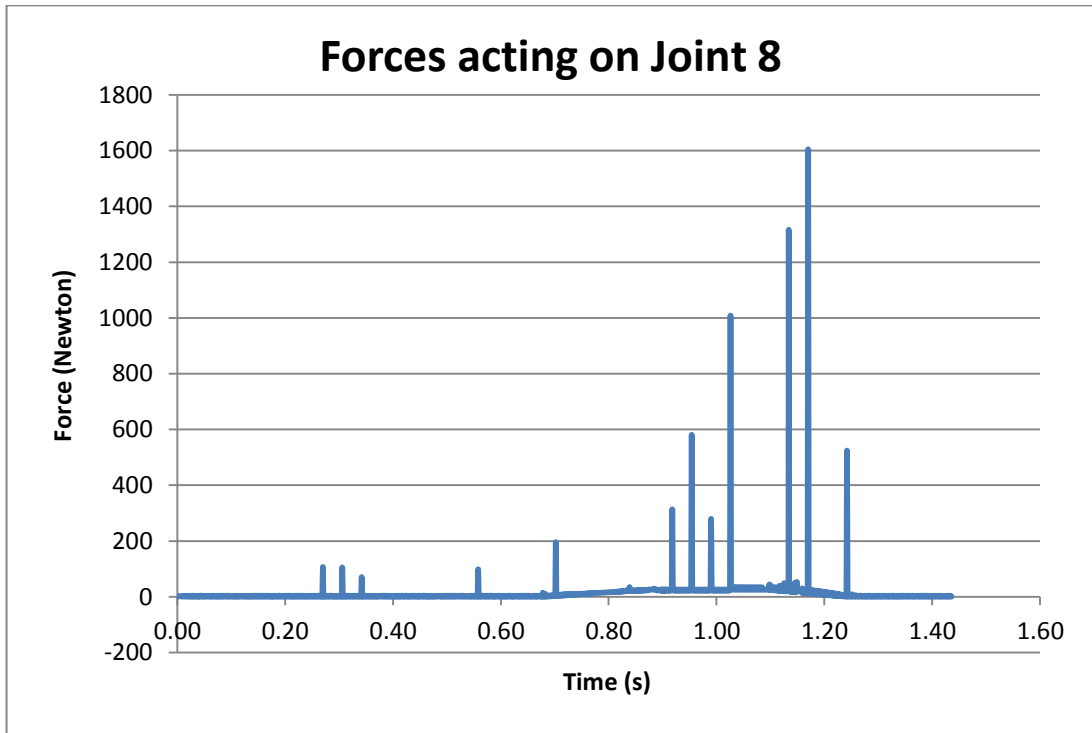
Figure 24 Kinematic Diagram with Joints

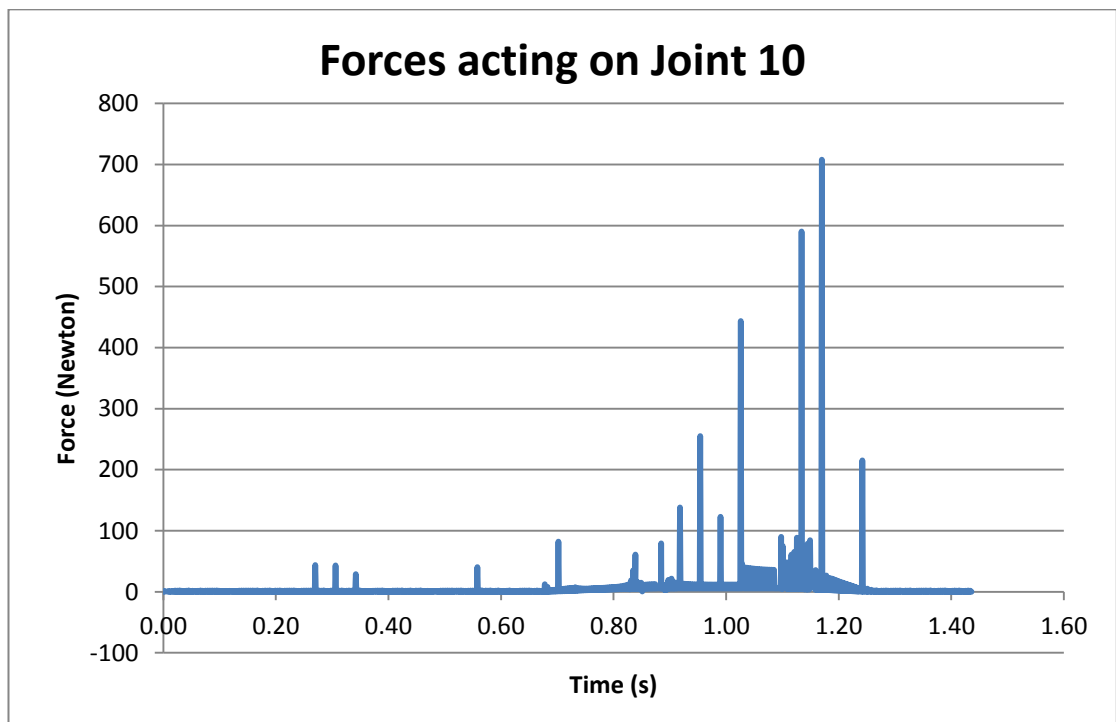












As can be seen from the graph shown for each joint, the forces vary with different values. Some of the joints like joint 3, joint 4, joint 5 and joint 6 do not show any significant values. This shows that the forces that act on these joints can be neglected. Different goes with joint 1. From the graph, it can be seen the force increase so rapidly between 1 to 1.4 sec and decrease rapidly again. This happens because during simulation, when the robot is moving from small diameter to big diameter, the joint that has the rear wheel is the only part that is in contact with the surface of the pipe. So the force will only be concentrated on that joint only.

This can also be seen on Joint 2 where the front wheel is attached. The force is almost linear in the bigger diameter and when it goes to smaller diameter, the force shows an increment and when the diameter gets bigger, it shows a decrement.

### 4.3.3 Velocity

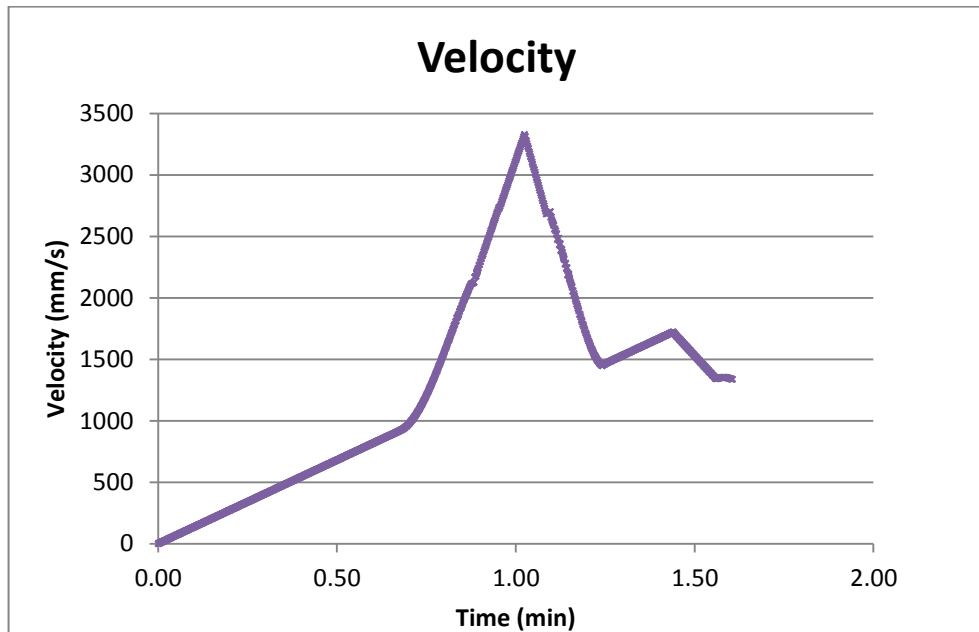


Figure 25 Velocity against Time

As seen from the graph obtained, the velocity of the robot increases with time and at a point it starts to decrease rapidly and again it increases again. This is because during the simulation, the motor is put only on the front wheel of the robot instead of at both wheels. The decrease in velocity of the robot occurs when the robot is transitioning from smaller diameter (6 inches) to bigger diameter (10 inches). During this transition, the front wheel of the robot does not have any contact with the surface of the and when it does, the speed starts to increase again. The motor of the robot should be put at both front and rear wheels but during simulation, when the motor is put in both wheels, the simulation failed.

Also, from the graph, it is observed the maximum speed of the robot is around 3300 mm/s or 3.30 m/s. This maximum speed is very high compared to the previous project which is around 0.15 – 0.30 m/s.

## **Chapter 5: Conclusion**

It can be concluded that all the objectives of this project has been successfully achieved. The robot has been designed and modeled accordingly and it satisfies all the limitations and constraints. The robot has also simple mechanism with less number of moving parts. It can also be seen that the robot will fit perfectly within pipe diameter ranging from 6 inches to 10 inches. The robot has also been simulated and the motion of the robot has been observed. Even though this project is feasible to be performed since the mechanical design of the robot is similar to the previous project, further research and study must be conducted in order to prove the legitimacy of this project.

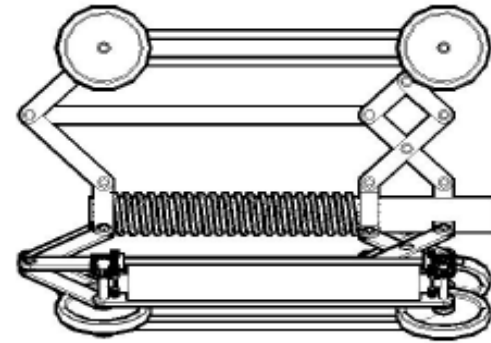
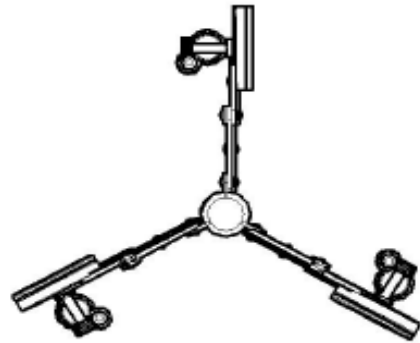
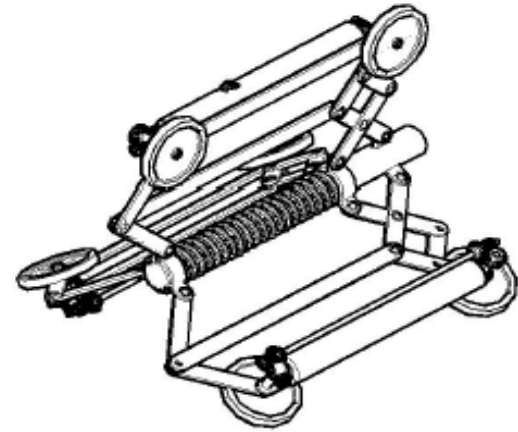
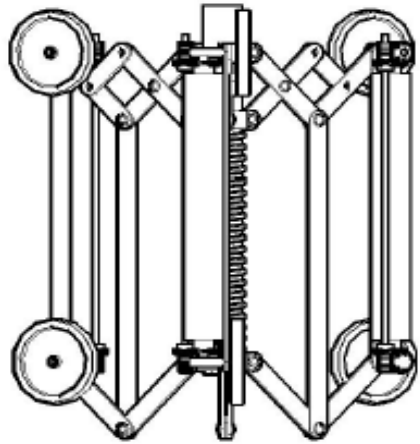
## References

1. O. Tatar, D. Mandru, I. Ardelean (2007). Development of mobile minirobots for in pipe inspection tasks. *MECHANIKA*. 60-64.
2. M. Horodinca, I. Doroftei, E. Mignon, A. Preumont (2002). A simple architecture for in-pipe inspection robots. *Proc. Int. Colloq. Mobile, Autonomous Systems*. 61-64.
3. K. Nishijima, Y. Sun, R.K. Srivastava, H. Ogai, and B. Bhattacharya (2010). Advanced pipe inspection robot using rotating probe. *The Fifteenth International Symposium on Artificial Life and Robotics (2010)*. 573-576.
4. W. Jeon, J. Park, I. Kim, Y.K. Kang, and H. Yang (2011). Development of high mobility in-pipe inspection robot. *SI International 2011*. 479-484
5. M. M. Moghaddam, M. Arbabtafti, and A. Hadi (2011). In-pipe inspection crawler adaptable to the pipe interior diameter. *International Journal of Robotics and Automation*. 135-145.
6. S.G Roh & H. R Choi (2005). Differential-drive in-pipe robot for moving inside urban gas pipelines. *IEEE Transactions on Robotics*, 21(1). 1-17
7. H. R. Choies & S. G Roh (2007). Bioinspiration and Robotics: Walking and Climbing Robots. *In-pipe Robot with Active Steering Capability for Moving Inside the Pipelines*. 375-402.
8. D. H. Myszka (2002). *Machines & Mechanisms : Applied Kinematic Analysis*, New Jersey: Pearson Prentice Hall.
9. C. Xu, X. Xie, & Y. Difan (2009). *Kinetic Drag Force Analysis of Micro In-Pipe Robot*. (641-645).

10. O. Tatar & D. Mandru (2008). Research Concerning Mobile Mini and Microbots. *Machine Design* (163-166).
11. Bekhit, A., Dehghani, A., & Richardson, R. (2012). Kinematic Analysis and Locomotion Strategy of a Pipe Inspection Robot Concept for Operation in Active Pipelines. *International Journal of Mechanical Engineering and Mechatronics*, 15 - 27.
12. H. Heidari, M. Mehrandezh, H. Najjaran and R. Paranjape (2010). *Design, Development, Dynamic Analysis, and Control of a Pipe Crawling Robot, Robotics 2010 Current and Future Challenges*, Housseem Abdellatif (Ed.), ISBN: 978-953-7619-78-7, InTech, Available from: <http://www.intechopen.com/books/robotics-2010-current-and-future-challenges/design-development-dynamicanalysis-and-control-of-a-pipe-crawling-robot>
13. Nisbett, J. K., & Budynas, R. G. (2008). *Shigley's Mechanical Engineering Design*. New York: McGraw-Hill.
14. Apostolopoulos, D. S. (2001). *A Thesis Degree of Doctors of Philosophy in Robotics: Analytical Configuration of Wheeled Robotic Locomotion*. Pittsburgh: Carnegie Mellon University.
15. Jr., J. O., Adamowski, J. C., Suzuki, M. S., Buiocchi, F., & Camerini, C. S. (1999). Autonomous System for Oil Pipelines Inspection. *Mechatronics*, 731-743.
16. Yukawa, T., Suzuki, M., Satoh, Y., & Okano, H. (2006). Design of Magnetic Wheels in Pipe Inspection Robot. *2006 IEEE International Conference on Systems, Man, and Cybernetics* (pp. 235-240). Taipei: IEEE.
17. Qiao, J., & Shang, J. (2012). Application of Axiomatic Design Method in In-pipe Robot Design. *Robotics and Computer-Integrated Manufacturing*, 49-57

18. Nise, N. S. (2008). *Control Systems Engineering*. Rosewood Drive: John Wiley & Sons, Inc.
19. Hibbeler, R. C. (2007). *Engineering Mechanics Dynamics*. Jurong: Pearson Prentice Hall.
20. K. Suzumori, T. Miyagawa, M. Kimura, Y. Hasegawa, “Micro Inspection Robot for 1-in Pipes” in *IEEE/ASME Transactions on Mechatronics*, vol. 4, No. 3, pp. 286-292. September 1999

## **APPENDICES**



In-Pipe Inspection Robot		
A4	Designed by Dr. Mark Dviris	Date 3/9/13
1 of 1		Rev A

